My Favorite Object

Eta Carinae and its ejecta, the Homunculus

Ted Gull

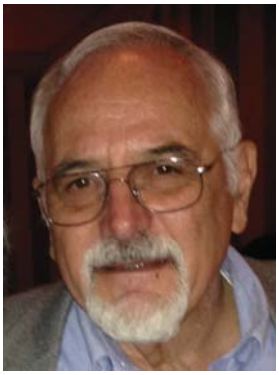

1 Motivation

Eta Carinae (η Car), its interacting winds and historical ejecta provide an unique astrophysical laboratory that permits addressing a multitude of questions ranging from stellar evolution, colliding winds, chemical enrichment, nebular excitation to the formation of molecules and dust. Every 5.54 years, η Car changes from high excitation to several-months-long low excitation caused by modulation of the massive interacting winds due to a very eccentric binary orbit. The surrounding Homunculus (Figure 1)and Little Homunculus, thrown out in the 1840s Great Eruption and the 1890s Lesser Eruption, respond to the changing flux, providing clues to many physical phenomena of great interest to astrophysicists.

Some, but certainly not all of the pressing questions concerning η Car include: 1) How did the massive binary drive out ten to forty $M_{\odot}$, yet survive?

2) Which star experienced the Great Eruption: the current massive primary, the less massive secondary, a third, now absent star?

3) Nitrogen is very overabundant with carbon and oxygen greatly depleted. Is this due entirely to the interrupted CNO-cycle or did molecule and dust formation contribute?

4) What is the dust that has formed? Is it alumina or silicon carbide, or metallic?

5) Why do we see emission and absorption lines of strontium, scandium and vanadium, elements not seen in the interstellar medium?

6) Are the winds stable or changing over the times longer than the 5.54-year cycle?

7) Are conditions in the shocked winds such that molecules and dust continue to form?

For the past sixteen years, I have participated with many interested astronomers in conducting multiple observations and modelings of this intriguing system. Many papers, conference proceedings and even several monographs [1] have been written about η Car. At conferences discussing massive stars and their final evolutionary stages, often η Car is the elephant in the room that some attendees prefer to ignore. Crucial observations to test and improve current models are scheduled during the next several months as the η Car drops from the five year long high excitation state to a several month interval of low excitation. In this discussion, I show what is so intriguing about this system and why we call it an astrophysical laboratory that lends itself well to studies of massive stars in late stages of stellar evolution, of massive, interacting winds, massive ejecta not yet mixed with the interstellar material, reaction of material to relatively high density shocks, high radiation levels and high densities.

While observations prior to the early 1800s are limited, observers noted that η Car brightened to exceed Canopus in the southern sky in 1838, stayed relatively bright for two decades, but then faded below naked-eye visibility. While η Car went through a minor brightening in the 1890s it again faded (Smith & Frew, 2011). Since the 1940s, η Car has experienced a gradual brightening achieving naked eye visibility in the last decade (for current photometry, see http://etacar.fcaglp.unlp.edu.ar/ Fernandez-Lajus et al., 2009).

Many observers have been quite intrigued with η Car. Gaviola (1950,1953) studied both the structure and spectra in the 1940's when astronomers noticed a gradual brightening that continues more or less to the present. Thaceray (1967) and Aller & Dunham (1966) obtained some of the first high dispersion spectra of the central source, identified many of the lines, described the broad and narrow profiles and noted changes in line profiles between observations approximately five years apart. Davidson et al. (1986) using ultraviolet spectra recorded by the itInternational Ultraviolet Explorer and visible spectra recorded by the Cerro Tololo Inter-American Observatory Blanco Telescope, determined that nebular nitrogen was very overabundant at the expense of carbon and oxygen. This suggested that within η Car is a very massive star capable of internal conduction leading to interruption of the CNO cycle leading to overproduction of nitrogen.

The central source is a massive binary whose periodicity

[1] A sub-sampling of reviews, conference proceedings and monographs includes: (Davidson & Humphreys, 1997; Gull, Johansson & Davidson, 2001; Davidson & Humphreys, 2012)

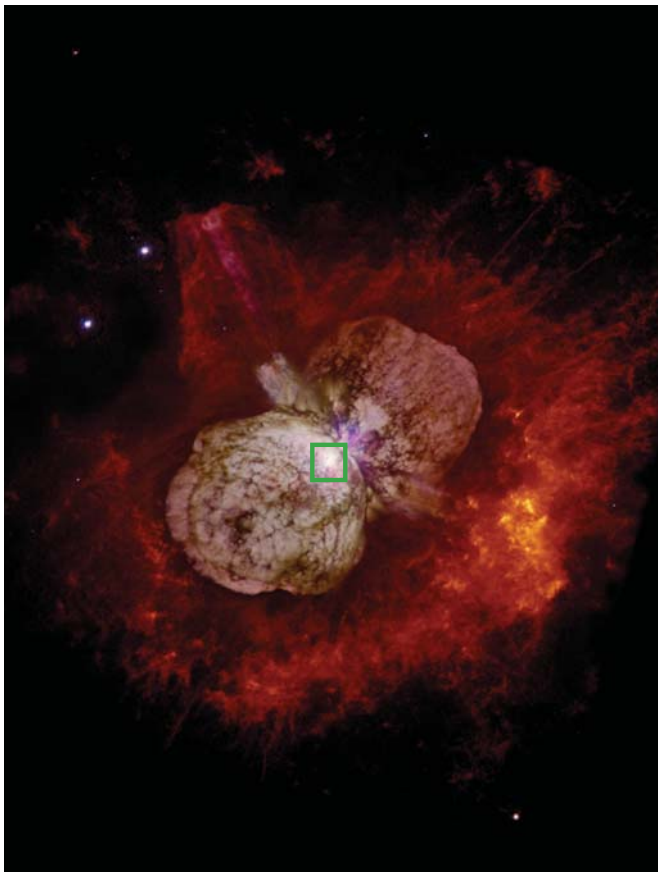

Figure 1: Hubble Space Telescope Image of η Car and the Homunculus. The Homunculus, a bi-lobed dusty shell measuring 10" × 20" on the sky originated in the 1838-1845 Great Eruption and is expanding at about 600 km s^{-1}. Outside the Homunculus expands even faster moving gas, also thought to originate from the 1840s event. This external gas was estimated by Smith (2008) to have space velocities as high as 4000 km s^{-1}, . Internal to the Homunculus is an ionized, bipolar Little Homunculus, discovered by Ishibashi et al. (2003) through mapping with the /hst//stis long slit. It originated during the 1890s Lesser Eruption. Field of view approximately 40". The area within the green box is displayed in Figure 2.

was first noticed by Augusto Damineli through the periodic weakening of He I 10830Å emission accompanied with fading of other He I lines and disappearance of [Ar III] every 5.52 years (Damineli, 1996). Previous observers had suggested much longer periods, limited by the very sparse spectroscopic data taken over the previous century. Payne-Gaposhkin (1957) al. (1998) refined the period to 2024 ± 1.7 days (5.54 years). They noted that both broad and narrow components of many forbidden lines of [Ne III], [Ar III], [Fe III], [N II], [Fe II] and [Ni II] were modulated by the 5.54-year period. Ultimately this periodicity was found to be associated with the period of a massive binary with a highly eccentric orbit. The FUV radiation from the hot, less massive secondary plunges within one to two AU of the primary, well within the very extensive primary wind, thus modulating the FUV and X-ray emission. Damineli et al. (1998) defined the broad high ionization state associable with the lengthy time spent with the binary at large separation as most of the orbit is spent at distances close to apastron and the short low-ionization state associable with the rapid, very close passage across periastron.

Hillier et al. (2001, 2006) modeled the *STIS* spectra using CMFGEN and determined that the primary star, η Car A, is at least 100 $M_{\odot}$. Based upon the excitation of Weigelt B and D, Verner et al. (2002) and Mehner et al. (2010) placed estimates of 30 to 50 $M_{\odot}$ for the secondary η Car B.

2 The System

Today we see a massive Homunculus, so named by Gavioli (1950) as the nebulosity had a humanoid appearance in seeing-limited photographic imagery. By the current decade, the Homunculus has an apparent size of 10" × 20" and with radial expansion velocities up at 600 km/s (Figure 1). With modern observatories and imaging spectrographs, spatially resolving structures within this ejecta prove to be quite feasible, thus enabling detailed studies of quite different physical conditions within the ejecta. Smith (2006) used long-slit spectra obtained with the Phoenix spectrograph on Gemini South to determine the distance to be 2350 ± 50 pc. Exterior structures, seen primarily in the red Hα+[N II] emission, also originated during the Great Eruption. Smith (2008) suggested that this material moves at space velocities between 3500 to 6000 km/s. Indeed kinetic energy expended during the Great Eruption of the 1840s must rival that of a weak supernova remnant. As the number of pseudo-supernova events in nearby galaxies accumulate, it becomes increasingly convincing that η Car is not unique, but rather the phenomenon that we have observed for nearly two centuries is a transient stage in the evolution of massive binary systems. This compels us to study η Car and its ejecta even more.

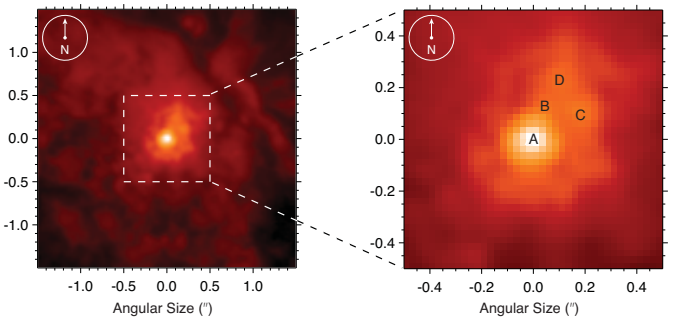

Figure 2 Left: Central 3" core of η Car and the Homunculus (*HST*/ACS F550M image). **Right:** Central 1" indicating η Car and the Weigelt condensations. The Weigelt condensations (labeled B, C and D) with intense narrow-line emission, additional condensations appear to form a ring around the central stellar component at a 0.25" radius. However, spectra of these condensations as seen by *HST*/STIS indicate scattered starlight and extended wind. This entire, complex region contributes to the spatially extended wind which *HST*/STIS resolves, but ground-based, visible spectroscopy cannot.

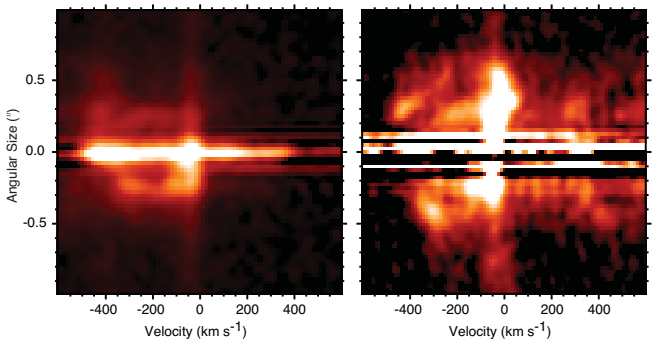

Figure 3 Left: Spectro-image of [Fe III] 4659Å recorded with *HSTSTIS*. While η Car shows bright [Fe III] emission extending from -450 to +350 km s^{-1}, a loop of emission extends from -0.2" to +0.2" and from -450 to 0 km s^{-1}. By contrast, the [Fe II] 4815Å emission shows multiple arcs extending form -0.6" to +0.6" and from -450 to +400 km s^{-1}. The [Fe III] arcuate structure was replicated by 3-D modeling when the orbital pole of the binary system was aligned to the axis of symmetry of the Homunculus, thus indicating a strong relationship between the binary system and the shape of the Homunculus (Madura 2010; Gull et al. 2009). Note the very bright [Fe II] emission at -40 km s^{-1} which originates from slow moving material, including the Weigelt blobs, thought to have been ejected in the Lesser Eruption in the 1890s.

2.1 Winds and Nearby Ejecta

Emission line structures located close to η Car are spatially and spectrally resolvable, especially with the *HST* angular resolution of 0.1" (235 AU) and the many spectral modes of the *STIS* (Woodgate, et al. 1998). Davidson et al. (1997) successfully proposed to use the *STIS* long slit capabilities to obtain spectra of the four point-like components first detected by Weigelt & Ebersberger (1986). While Weigelt A is the stellar η Car, the other three components are very bright, highly-excited, somewhat-extended, emission nebulae, located within hundreds of AU of η Car (see Figure 2). This led to a series of programs utilizing the spectral and spatial capabilities of *HST* with *STIS* that addressed the variability of η Car and the responses by the Weigelt blobs and other ejecta across the broad high ionization state and the brief low ionization state. The first series of observations captured spectra of η Car during the 1998.0 low state (binary system near periastron) and later observations in the first few years of the high state (Davidson et al. 1997; Gull et al. 1999; Davidson et al. 1999). A collaborative *HST* Treasury program (Davidson et al. 2001, 2003) provided detailed spectroscopic studies of η Car and selected structures of the Homunculus from Lyα to one micron. Zethson (2001), Zethson et al. (2012) identified nearly two thousand narrow emission lines in the *STIS* moderate dispersion spectra of Weigelt B and D. While most lines originated from singly ionized species such as Fe^{+}, narrow emission lines also were identified from Fe^{++} and even Fe^{+++} (Zethson, 2001).

Several unanticipated discoveries resulted from the *STIS* long slit observations. A limiting factor of *HST* is that the solar panels must always be oriented towards the Sun. Hence the position angle of the long slit on the *STIS* has a bounded range that varies with time of the year. As our primary focus was on variations of η Car and secondarily on the Weigelt B, C and D, spectra of the emission blobs were obtained only when the slit orientation happened to include them or by additional spectra with specific offsets when necessary. Serendipity led to the detection of narrow, high-velocity, forbidden emission lines ultimately associated with the multiple shells created by the wind-wind interactions (Gull et al. 2009), an ionized bipolar structure associable with the Lesser Eruption of the 1890s (Ishibashi et al, 2003) and a very peculiar ionized metal region (Zethson et al., 2001).

Each long slit spectrum centered on η Car included weak forbidden line emissions components at velocities ranging from -450 to +400 km s^{-1} even when Weigelt B, C or D were not intercepted by the slit position. These narrow components changed with position angle, date of observation and ionic species. Lines of [N II], [Fe III], [S III], [Ar III] and [Ne III] showed components from -450 to 0 km s^{-1} across the broad high state that disappeared during the low state. In contrast, lines of [Fe II] had velocity components from -450 to +400 km s^{-1} during the

high state, but increased to include -400 to +400 km s^{-1} within the low state. An example is presented in Figure 3 of [Fe III] and [Fe II] extracted from the same spectrum centered on η Car. These fainter, red-shifted and blue-shifted narrow line emission structures ultimately proved to be spatially resolved structures caused by the interacting winds (Gull et al. 2009).

An earlier attempt to characterize the binary system using the *STIS*-derived velocity shifts of the He I absorption in the apparent P-Cygni line profiles led to the realization that the He I absorption originates from near the apex of the wind-wind interaction zone (Nielsen et al. 2007). The He I profiles and forbidden emission lines led to three-dimensional hydrodynamic modeling of the interacting winds that led to quantifying the properties of the massive interacting winds (Madura 2010), determining that the orientation of the binary orbital axis is closely aligned to the axis of symmetry of the Homunculus (Madura et al. 2012) and more recently placing limits on how much the properties of the winds have changed over the past few cycles (Madura et al. 2013).

2.2 The Intermediate Ejecta

As with Alice examining Wonderland, the more that η Car and the Homunculus are observed, the results became curiouser and curiouser. The physical conditions of the Homunculus are quite varied. Mapping with the *HST/STIS* of the central four arc seconds in the Hβ spectral region revealed an internal, ionized bipolar shell, seen in multiple [Fe II] and other emission lines, that was ejected in the 1890s during the Lesser Eruption (Ishibashi et al 2003) .

Likewise, mapping near the Hα spectral region revealed a very curious emission line region. Located about 2" north of η Car, the structure was first identified by [Sr II] at -110 and -100 km s^{-1} velocities (Zethson et al. 2001). Subsequent *HST/STIS* spectra revealed many more forbidden emission lines, most notably of [Ti II] but no hydrogen, oxygen or carbon emission lines (Hartman et al 2004). Analoguous to the classical HII region, ionized by Lyman continuum, this region is excited by radiation that has been filtered by Fe^+ in the primary wind to energies less than about 8 eV. Hence hundreds of emission lines appear from many singly ionized metals including Ti^+, Sr^+, V^+, Sc^+, i.e. species not usually seen in HII regions for two reasons: the species are either ionized to higher states, or more likely the species have combined with carbon or oxygen to form molecules and eventually build on dust grains. The carbon and oxygen is so depleted that these species are left in atomic and singly-ionized states.

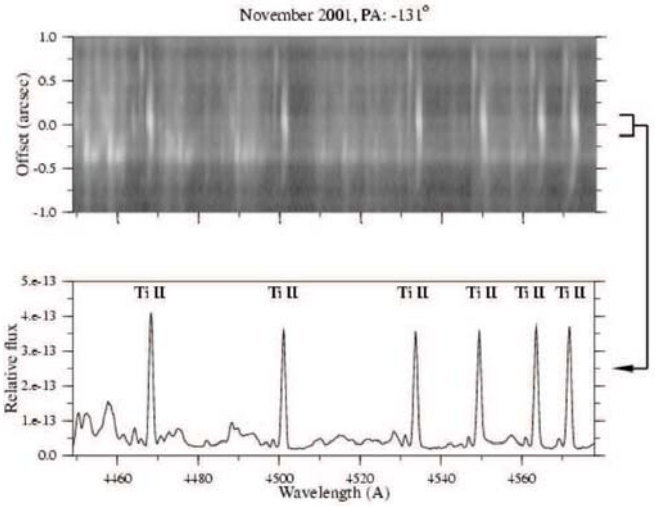

Figure 4 Top: Spectro-image of the Strontium Filament from 4450 to 4580Å. **Bottom:** Tracing at the central position with demonstrating that the six bright lines identified with Ti^+ (Hartman et al. 2004).

2.3 The Homunculus

The Homunculus, a dusty, bipolar shell expanding at 600km s^{-1}, contains considerable material. The total mass of the Homunculus is difficult to quantify simply because of the huge range in velocities and the strange dust with high polarization and grey scattering properties. While estimates of the total mass have been derived based upon the infrared emission, the assumption of a gas to dust ratio being 100/1 is not supported. The dust grains formed from the Great Eruption were formed at high temperatures and have not cooled to the low temperatures of the ISM. They likely do not have ice mantles. Line of sight studies using the bright source, η Car, revealed a plethora of narrow absorption lines, mostly at -513 km s^{-1} originating from a thin inner surface of the expanding shell (Gull et al 2005; Nielsen et al. 2005). Multiple additional absorption velocities were noted in singly-ionized species including the -146 km s^{-1} component associable with the Little Homunculus. Most ranged at 10 to 20 km s^{-1}intervals between -585 to -380km s^{-1}. Likely they are due to changes of primary wind velocity in line of sight from cycle to cycle since the Great Eruption, or evidence of long term changes in the primary wind velocity.

The -513 km s^{-1} velocity component is seen in both ionic and molecular species. Approximately a thousand ionic absorptions were identified from $Mg^+, Mn^+, Ti^+, V^+, Sc^+, Sr^+, Fe^+$. As many lines of these ions originate from levels above the ground state, we characterized the ion gas temperature to be 760°K. Over 800 H_2 absorption lines were observed coincident at the same velocity. In addition, combining *HST/STIS* and *VLT/UVES* spectra,we detected CH, OH

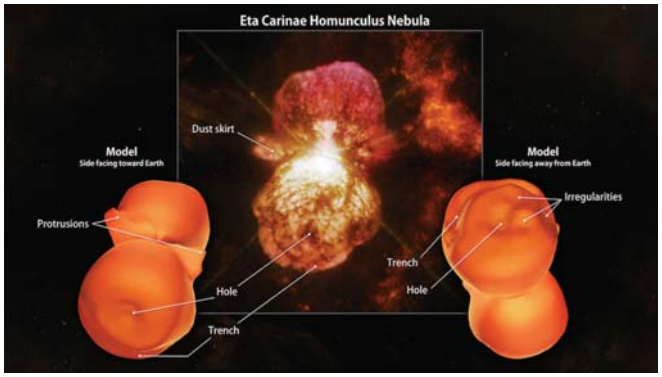

Figure 5 Top: 3-D model of H_2 as derived from *VLT/XShooter* spectroscopic mapping of the 2.12μ emission line (Steffen et al. 2014, MNRAS July 8 issue). The bipolar lobes are distorted from the idealized hourglass shape: 1) a hole exists at the pole of each lobe, 2) a trench is seen on one side of each lobe, being point symmetrical from η Car 3) two protrusions are located near the central region, but tilted relative to the dust skirt and to the previously inferred orbital plane of the binary, and 4) no H_2 is detected in the dusty skirt as noted by Smith (2006).

and NH ground state absorptions but no CO. Quasithermal arguments would suggest that the molecular gas was cooler that 40^{o}K. The H_2 absorptions are the result of electronic photo-excitation to upper levels with cascades down through many levels. Intriguingly the H_2 absorptions disappeared during the low state, confirming that the FUV radiation was cut off during the periastron event within the Homunculus. Deep to the interior Little Homunculus, multiple, very strong Ti^+ (13.8 eV ionization potential) absorptions appeared at -146 km s^{-1} during the minimum, also confirming that the FUV was cut off within that smaller structure!

Observations with Herschel contain a number of molecular emission lines with multiple velocity components. Indeed molecular studies of the Homunculus are compounded by the huge velocity range form -600 to +600 km s^{-1} that 1) requires very large velocity coverage and 2) high angular resolution meeting and exceeding the 0.1" angular resolution of *HST*. Strong clues are provided by the Herschel data (Gull et al, 2014 in prep) and promise much new, exciting results when and if ALMA time is granted.

An overall effort continues to characterize the Homunculus. Recently a complete spectroscopic mapping was accomplished with the *VLT/XShooter* and a 3-D model was derived using the H_2 2.12 μ emission line (Steffen et al, 2014, MNRAS, July 8 issue). Figure 5 depicts two views of the model as seen from Earth and as seen on the far side. Distortions from the bipolar structure indicate influence by the binary system at the time of the Great Eruption and possibly since the eruption.

3 The 2014.6 Periastron Event

Each of the last three periastrons has been followed with increasing interest as improved models of the binary system, especially of the interacting winds are built in parallel with new observatories and instruments coming online. Indeed one major problem has been that ground-based telescopes and their instrumentation are upgraded/replaced often enough that no more than two periastron passages are observed by the same instrument. While the 1998.0 and 2009.1 passages were optimal for monitoring with night observations near the meridian, the 2003.5 and the upcoming 2014.6 passage occurs while the meridian passage of η Car is in daytime. Hence, good monitoring from the ground is more achievable every alternate cycle, or eleven years. Space observatories and their instrumentation tend to be used for longer intervals. The itInternational Ultraviolet Explorer Observatory provided seventeen years of intermittent, proposal-dependent coverage, but occurred from 1978 to 1986, well before the 5.54-year period was discovered (Damineli 1996). Moreover, the 3" aperture and the 10"$\times$20" oval aperture did not provide separation of the stellar flux from the nebular-scattered and emitted fluxes. The optimally-matched imaging capabilities of the *STIS* to the *HST* proved ideal for the study of η Car and the Homunculus. Much more has been possible during the times when the *STIS* has been operational since 1998. However, the *STIS* experienced an electronic failure in early 2004 that extended to early 2009 but was repaired during the Servicing Mission 4 in May 2009. Discovery that the interacting winds could be traced has provided considerable new knowledge about how massive winds interact. The first spectra taken with *HST/STIS* after the Servicing Mission 4 was a demonstration mapping focused on measuring the extended wind interactions. One long slit spectrum from that mapping activity provided input to the graphic demonstrating the powers of imaging spectroscopy in Figure 6.

This mapping activity demonstrated the ability to map with *HST/STIS* of structures 2" on the side and led to successful programs designed to map the extended wind structures over the current 5.54-year cycle in coordination with several X-ray observatories and multiple ground-based observatories. Currently we have followed the wind structures for the five years of the high (apastron) state. In a paper in preparation (Gull et al. 2014), slow, predictable changes are detected. Red-shifted shells in [Fe II] expand outward at 470 km s^{-1} (Teodoro et al. 2013). Blue-shifted arcs move outward as similar speeds . Light house effects on the wind structures are traceable caused by the sweeping of FUV radiation as the secondary star moves in orbit carving a cavity in the massive primary (Gull et al. in prep).

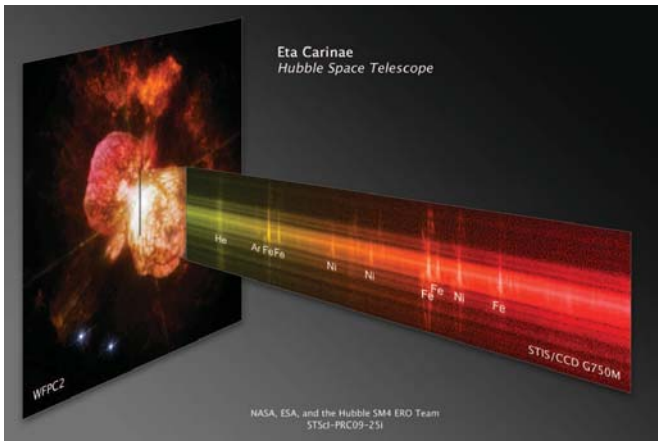

Figure 5 Graphic derived from the first set of observations with*HST*/*STIS* after *STIS* repair during the shuttle Servicing Mission 4 in May 2009. On the left is an *HST*//it WFPC2 image with a projected *STIS* 0.1"-wide aperture extending about eight arc seconds. Extending outward from the image is a color (arbitrary)-encoded spectrum from 7000 to 7700Å. The vertical features labeled He, Ar, Fe, Ni are nebular emission from a portion of the interacting winds, the Little Homunculus and the Homunculus.

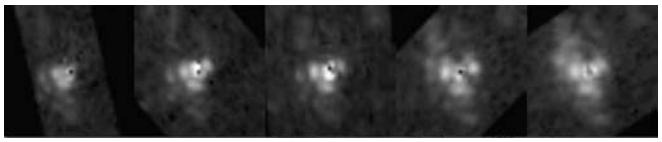

Figure 7: Mapping the winds of η Car A velocity slice of [Fe II] 4815Å at a red-shifted velocity. The shells to the southeast of η Car are residual structures originating from the 2009.1, the 2003.5 and the 1998.0 wind-wind interactions. Teodoro et al (2013) found that these shells expand at 470 km s^{-1}, about ten percent higher than the independently measured primary wind velocity of 420 km s^{-1} (Groh et al. 2012).

η Car, through the monitoring of He I 6678Å narrow line emission, is predicted to enter the low state associated with the periastron passage on or about July 26 (Augusto Damineli, private communication). A few weeks later the X-ray flux, being monitored by SWIFT (Michael Corcoran) will disappear. The latest mapping with *HST*/*STIS* on June 7, 2014 already indicated initial decline in total flux and shrinkage of various [Fe III] 4659Å structures along with increasing total flux and expansion of [Fe II] 4815Å structure. Ground-based spectroscopy, coordinated by Augusto Damineli, Mairan Teodoro and Noel Richardson, likewise are indicate changes are beginning as predicted. Ground-based photometry is continuously coordinated by Eduardo Fernando-Lajus (see http://etacar.fcaglp.unlp.edu.ar/).

Mapping visits with *HST*/*STIS* are scheduled for early August, and November of 2014 and mid-January, 2015 to measure the rapidly changing structures across periastron and recovery. Very little [Fe III] emission will be present in the outer shells by August when η Car is in the depths of the low state. In contrast, virtually all shells, excited by mid-UV from the primary star and collisions, will be visible in [Fe II]. By November, some [Fe III] emission from the innermost shells should be present and by January more shells will again be visible in [Fe III]. Ground-based spectroscopy will fill in the gaps between mappings showing how and when different velocity components again see the FUV radiation leading to doubly-ionized iron.

In parallel, X-ray spectroscopic observations are scheduled with CHANDRA, Suzaku, SWIFT and NuSTAR at critical times to increase understanding of the most energetic shock activity (Kenji Hamaguchi and Michael Corcoran).

Critical to all of these observations are the 3-D hydrodynamical models that have been carefully developed by Madura et al. (2013). This paper provides predictions to be tested by the observations. The models are based upon the best estimates for the wind properties and predict at what phases changes should be occurring based primarily on the best estimate of the primay mass loss rate and potentially decreased mass loss rates. η Car has continued to gradually brighten, Hα flux has declined relative to continuum, and the 2009.1 X-ray minimum was half in time relative to the 1998.0 and 203.5 minima. These changes suggest that the primary wind mass loss rate is declining, but by how much. Madura's models predict when changes should occur both in the decline and recovery, and based upon these predictions we should be able to constrain how much the winds have changed over the past three cycles.

However, η Car has always has a few surprises being held back. Will the anticipated changes take place as predicted? Do we know the physics well enough? Is the system stable or about to go through another major eruption?

Stay tuned!

4 Acknowledgements

I thank the many collaborators for very enjoyable discussions and shared papers that result on this fascinating object. I especially thank the η Car lunch-bunch who meet nearly daily at the Building 34 cafeteria at Goddard Space Flight Center.

Support for multiple programs using the *HST* was provided by NASA through a grants from the Space Telescope Science Institute, which is operated by the Association of Universities for Research in Astronomy, Inc., under NASA contract NAS 5-26555.

References:

Aller L. H., Dunham T. J. 1966, ApJ, 146, 126
Damineli A., 1996, ApJL, 460, L49
Damineli A., et al. 1998, A&AS, 133, 299
Damineli A., et al. 2008, MNRAS, 384, 1649
Davidson K., et al. 1986, ApJ, 305, 867
Davidson K., Humphreys, R. 1997, ARA&A, 1
Davidson K., et al. 1997, HST Program 7302
Davidson K., et al. 1999, HST Program 8337
Davidson K., et al. 2002, HST Program 9427
Davidson K., et al. 2003, HST Program 9973
Davidson K., Humphreys R. M., eds, 2012, Eta Carinae and the Supernova Impostors Vol. 384 of Astrophysics and Space Science Library
Fernandez-Lajus E. et al. 2009, A&A, 493,1093
Gaviola E., 1950, ApJ, 111, 408
Gaviola E., 1953, ApJ, 118, 234
Groh J.H., et al 2012, MNRAS, 423, 1623
Gull T.R., et al. 1999, HST Program 8036
Gull T. R., Johannson S., Davidson K., eds, 2001, Eta Carinae and Other Mysterious Stars: The Hidden Opportunities of Emission Spectroscopy. Vol. 242 of Astronomical Society of the Pacific Conference Series
Gull, T. R. et al. 2005, ApJ, 520, 242
Gull, T. R. et al. 2009, MNRAS, 396, 1308
Hartman H., et al, 2004, A&A, 419, 215
Hillier D. J., et al. 2001, ApJ, 553, 837
Hillier D. J., Gull T., Nielsen K., et al. 2006, ApJ, 642, 1098
Ishibashi K., et al. 2003, AJ, 125, 3222
Madura, T. I. 2010, PhD thesis , University of Delaware
Madura, T. I. 2012, MNRAS, 420, 2064
Madura T. I., et al. 2013, MNRAS, 436, 3820
Mehner A., et al. 2010, ApJ, 710, 729
Nielsen K. E. et al, 2007, ApJ, 660, 669
Nielsen K.E. et al. 2005,, ApJS, 157, 138
Payne- Gaposchkin, C. 1957, The galactic novae.. North-Holland
Smith N., 2006, ApJ, 644, 1151
Smith N., 2008, Nature, 455, 201
Smith N., Frew D. J., 2011, MNRAS, 415, 2009
Teodoro M., et al. 2013, ApJL, 773, L16
Thackeray A. D., 1967, MNRAS, 135, 51
Verner E. M., et al. 2002, ApJ, 581, 1154
Weigelt G., Ebersberger J., 1986, A&A, 163, L5
Woodgate B. E., et al. 1998, PASP, 110, 1183
Zanella R., Wolf B., Stahl O., 1984, A&A, 137, 79
Zethson T., 2001, PhD thesis, Lund University
Zethson T. et al. 2001 AJ, 122, 322
Zethson T., et al. 2012, A&A, 540, A133